LETTERS

Interdimensional universality of dynamic interfaces

Kab-Jin Kim[1], Jae-Chul Lee[1,2], Sung-Min Ahn[1], Kang-Soo Lee[1], Chang-Won Lee[3], Young Jin Cho[3], Sunae Seo[3], Kyung-Ho Shin[2], Sug-Bong Choe[1] & Hyun-Woo Lee[4]

Despite the complexity and diversity of nature, there exists universality in the form of critical scaling laws among various dissimilar systems and processes such as stock markets[1], earthquakes[2], crackling noise[3], lung inflation[4] and vortices in superconductors[5]. This universality is mainly independent of the microscopic details, depending only on the symmetry and dimension of the system. Exploring how universality is affected by the system dimensions is an important unresolved problem. Here we demonstrate experimentally that universality persists even at a dimensionality crossover in ferromagnetic nanowires. As the wire width decreases, the magnetic domain wall dynamics changes from elastic creep[6–9] in two dimensions to a particle-like stochastic behaviour[10] in one dimension. Applying finite-size scaling, we find that all our experimental data in one and two dimensions (including the crossover regime) collapse onto a single curve, signalling universality at the criticality transition. The crossover to the one-dimensional regime occurs at a few hundred nanometres, corresponding to the integration scale for modern nanodevices.

The universality manifests in the self-organized scale-invariant scaling behaviour of metastable states with huge degrees of freedom. This scaling behaviour is inevitably related to the system dimensions and so we wished to explore the scaling criticality for different dimensions and to clarify the interlinking between them. Much theoretical work has been devoted to clarifying universality classes in various dimensions[11–15] but experimental evidence has been lacking for low-dimensional systems because signals from small specimens become harder to detect as the dimension reduces. Recently, however, two-dimensional (2D) systems have been successfully studied using magneto-optical Kerr effect (MOKE) microscopy on ferromagnetic thin films, manifesting the Barkhausen criticality[16] and its tunability with temperature[17]. Another experimental test in two dimensions involves scaling criticality in the creep motion of a magnetic domain wall (DW) driven by a weak magnetic field[6–9]. Excellent agreement is found with the theoretical formula[6,7] predicting the collective DW motion. Starting from this well-established 2D creep criticality, here we demonstrate that the criticality in ferromagnetic nanowires exhibits universal transition behaviour from two dimensions to one as the wire width decreases. The transition threshold is revealed to be determined solely by the ratio between the wire width and the length of the DWs that move together. Below the transition threshold, the nanowires exhibit another distinct scaling behaviour of one-dimensional (1D) DW hopping criticality[10].

Nanowires of various widths ranging from 4 μm to 150 nm were patterned by electron-beam lithography and ion milling onto a 5.0-nm Ta/2.5-nm Pt/0.3-nm $Co_{90}Fe_{10}$/1.0-nm Pt film with perpendicular magnetic anisotropy. The dynamic DW criticality was investigated by monitoring the DW propagation speed generated by a magnetic field. The nanowires were initially saturated under a sufficiently large magnetic field and then a reversed domain was formed by thermomagnetic

writing on the nanowires under a small reversed field. The DW arrival time after applying a magnetic field was then measured at a position 40 μm away from the initial DW position by means of MOKE detection. The arrival times observed spanned more than four orders of magnitude (10 ms to 1,000 s) while we varied the strength of the magnetic field.

We observed a distinct transition from the 2D creep criticality with decreasing wire width w. In two dimensions, the DW propagation speed V follows the form of the creep scaling criticality[7] with respect to the applied magnetic field H according to $V(H) = V_0\exp(-\alpha H^{-\mu})$. Here, V_0 is the characteristic speed and α ($= U_C H_{crit}^{\mu}/k_B T$) is a constant related to the scaling energy constant U_C, the critical magnetic field H_{crit}, and the thermal fluctuation energy $k_B T$. The scaling exponent μ is solely determined by the dimensionality of the system and the DW roughness. In 2D systems, it has been theoretically predicted[7] and experimentally verified[6] that μ equals 1/4. Figure 1 shows the plot of $\ln(V)$ versus $H^{-\mu}$ for nanowires of various widths. The linear dependence in Fig. 1a–c clearly demonstrates that wide wires ($w \gtrsim 600$ nm) exhibit typical 2D creep behaviour. However, for wires narrower than 500 nm, the data begin to deviate from the 2D linear
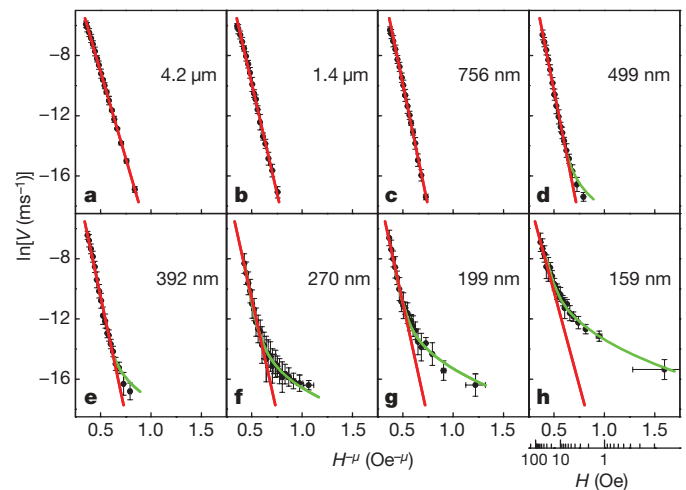
Figure 1 | Nonequilibrium criticality of DW speed along ferromagnetic nanowires. Data are shown for different wire widths: 4.2 μm (**a**), 1.4 μm (**b**), 756 nm (**c**), 499 nm (**d**), 392 nm (**e**), 270 nm (**f**), 199 nm (**g**) and 159 nm (**h**). The symbols show averaged values of ten repeated measurements for each H. The error bar (ordinate) is the standard deviation of the time measurements plus the maximum inaccuracy of initial DW positions. The error bar (abscissa) is ±0.15 Oe corresponding to the inaccuracy of the H measurement. The scale bar beneath panel **h** shows the values of H. The red lines are the best fit to the 2D criticality ($\mu = 1/4$ is used) and the green lines are the best fit to the 1D criticality given by equation (1).

[1]Center for Subwavelength Optics and School of Physics and Astronomy, Seoul National University, Seoul 151-742, Korea. [2]Center for Spintronics Research, Korea Institute of Science and Technology, Seoul 136-791, Korea. [3]Samsung Advanced Institute of Technology, Yongin 449-712, Korea. [4]PCTP and Department of Physics, Pohang University of Science and Technology, Pohang, Kyungbuk 790-784, Korea.

behaviour and finally, completely distinct behaviour appears in Fig. 1f–h for $w \leq 300$ nm.

A standard scaling treatment is adopted to examine the crossover between these distinct scaling behaviours. All the data shown in Fig. 1 are replotted onto a single plot in Fig. 2a with scaling axes where the abscissa is $\alpha H^{-\mu}$ and the ordinate is $\ln(V/V_0)$. The values of α and V_0 are experimentally determined from the best fit for each wire (the red lines in Fig. 1). In Fig. 2a, all the data are collapsed onto a straight line with different thresholds for the upward deviations. The threshold values turn out to depend primarily on the ratio of the wire width to the collective DW length L_{col}. Here, L_{col} is the length of a DW segment that thermally jumps over the quenched disorder potential collectively and gives rise to the creep motion. According to ref. 6, $L_{col} = L_C[u_C\mu/2\xi(\mu+1)]^{(2+\mu)/3}(H_{crit}/H)^{(2+\mu)/3}$ (Supplementary Information V), where the Larkin length $L_C = (\sigma\xi/M_S H_{crit})^{1/2}$ is the DW segment length ($<L_{col}$) above which effects of the disorder potential become dominant over the DW elasticity. Here σ is the DW energy density per unit area, M_S is the saturation magnetization, ξ is the correlation length of the disorder potential, and u_C is the roughness of the DW segment with length L_C. We note that L_{col} is proportional to a negative power of H and thus, for a sufficiently small field L_{col} becomes larger than the

wire width. When $L_{col} > w$, it is reasonable to expect that the collective DW segment length becomes w instead of L_{col} and the 2D criticality breaks down. Shorter collective segments experience a smaller energy barrier[6], so this replacement of L_{col} by w boosts the DW speed and the scaling curve is consequently bent upward. The regime of the 2D criticality is therefore bounded by the ratio w/L_{col}, explaining why narrower wires exhibit larger deviation from the 2D criticality.

Strikingly, all the data collapse onto a universal crossover curve when w/L_{col} is chosen as the abscissa and $\ln(V_0/V)/\alpha H^{-\mu}$ as the ordinate (Fig. 2b). The values of L_{col} used in the plot are estimated by assuming[6] $u_C \approx \xi \approx 10$ nm and $\sigma \approx 10$ mJ m^{-2} and using the experimental values $M_S = 1.7$ T and $H_{crit} \approx H_p$. The Bloch wall energy density σ is estimated using the typical values of the magnetic anisotropy 5×10^5 J m^{-3} and the exchange constant 1.3×10^{-11} J m^{-1}. Here, H_p is the DW propagation field, as discussed below. The collapse onto a single curve is good evidence for the universality of the criticality transition and the existence of a finite-size scaling function with w/L_{col} as a single governing parameter. The criticality transition exhibits gradual, rather than abrupt, crossover behaviour from the 2D criticality to another universal criticality. We verify that a simple change of μ cannot explain this new criticality (Supplementary Information IV).

One-dimensional criticality successfully explains the new criticality. In a true 1D structure, the DW has zero dimension and should behave as a particle. In addition, there is no way of detouring around pinning sites and so the DW can propagate only by hopping over the pinning sites. Therefore, we adopt a 1D model[10] that treats the DW as a particle stochastically hopping back-and-forth over a quenched disorder potential. The average DW speed at steady state under an applied field H is then given by $V(H) = (<\Delta x_n>/<1/W_n^+>)(1 - <W_{n+1}^-/W_n^+>)$, where $W_n^{\pm}$ is the rate of jumping from a pinning site n to a neighbouring pinning site $n \pm 1$ per unit time and Δx_n is the distance between the sites n and $n+1$. The equation is generalized from the original theory[10] by allowing the random distribution of not only $W_n^{\pm}$ but also Δx_n. We verify that V involves only the decoupled separate averages of the two quantities. Here, $< >$ denotes the average over all the sites n, because in general pinning sites are not identical. For the simplest case with all sites identical, the equation is simplified to $V = \Delta x(W^+ - W^-)$. We note that even when the DW is driven in one particular direction (say, $W^+ > W^-$), there exists a finite probability for a DW to hop in the reverse direction. Although this reverse motion is not important in the 2D regime, it turns out that it cannot be ignored in the 1D regime. In the thermally activated process, $W^{\pm}(H)$ becomes $f_0\exp(-E_B^{\pm}(H)/k_B T)$ according to the Arrhenius law, where f_0 is the attempt frequency and $E_B^{\pm}$ is the energy barrier. For small H, we use the Taylor expansion to obtain $E_B^{\pm}(H) = a_0^{\pm} + a_1^{\pm}H + \frac{1}{2}a_2^{\pm}H^2$, where $a_m^{\pm} = \partial^m E_B^{\pm}/\partial H^m|_{H=0}$. (Incidentally, the Taylor expansion is not allowed in the 2D regime because the energy barrier is singular at $H = 0$.) The inversion symmetry of the wire and magnetic field provides the symmetry relations $a_n^+ = (-1)^n a_n^-$ between the Taylor coefficients. The DW speed is then finally given to be:

$$V(H) = 2\Delta x f_0 \exp\left(-\frac{a_0^+ + \frac{1}{2}a_2^+ H^2}{k_B T}\right)\sinh\left(\frac{|a_1^+|H}{k_B T}\right) \quad (1)$$

The green lines in Figs 1 and 2 show the best fit to equation (1). This absolute theoretical conformity with all the experimental data provides strong evidence of the 1D criticality.

The Taylor coefficients in equation (1) have clear physical meanings in view of the conventional theory of thermally activated magnetization process[18–20]. The zeroth-order coefficient $a_0^{\pm}$ is closely related to the thermal stability of data storage with the retention time $\tau = f_0^{-1}\exp(a_0^{\pm}/k_B T)$. The first-order coefficient $a_1^{\pm}$ corresponds to $\mp V_A M_S$. The activation volume V_A is the characteristic volume acting as a single particle during the magnetization process, which is
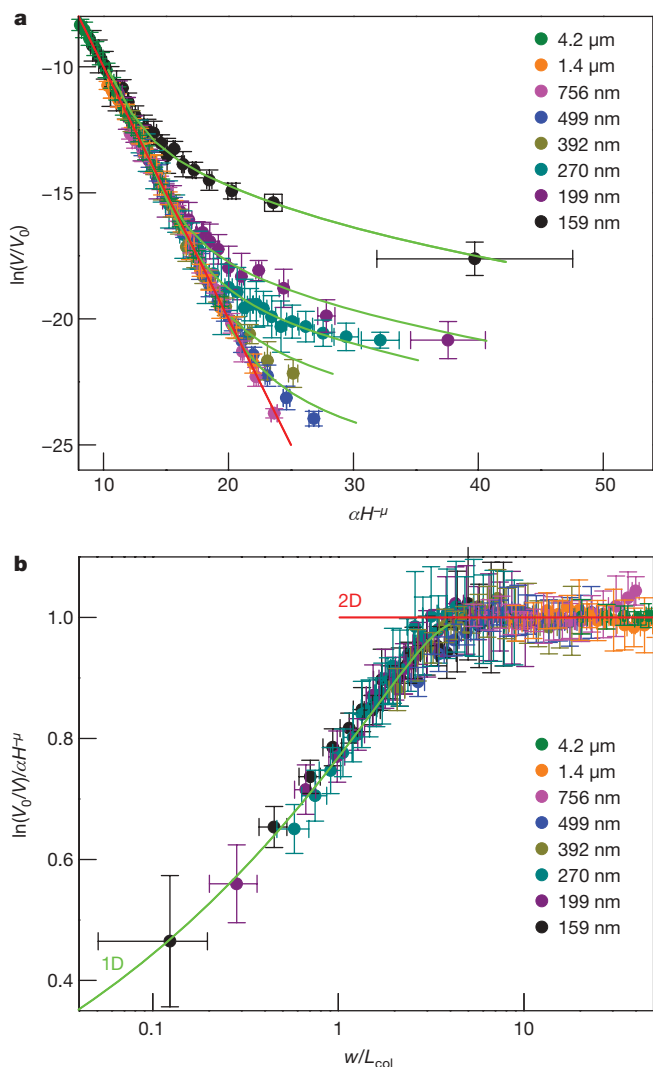
Figure 2 | Finite-size scaling and universal crossover behaviour of DW criticality. Scaled plots with $\ln(V/V_0)$ versus $\alpha H^{-\mu}$ (**a**) and $\ln(V_0/V)/\alpha H^{-\mu}$ versus w/L_{col} (**b**). In both panels, the symbols with different colours correspond to different wire widths as shown. The error bars are the same as those in Fig. 1. The red and green lines are the best fit to the 2D and 1D criticalities, respectively.
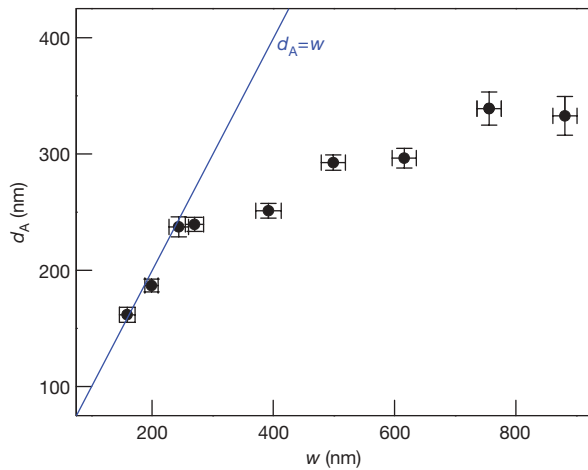
Figure 3 | Variation of activation diameter with respect to wire width. The symbols show the activation diameters d_A from the best fit to 1D criticality. The error bars correspond to the standard error in the χ-square fitting (ordinate) and the wire width variation (abscissa), respectively. The blue line guides the eye for $d_A = w$.

also related to the hopping distance Δx. The second-order coefficient $a_2^{\pm}$ is seen in the uniaxial magnetic anisotropy model[19] as $a_2^{\pm} = (a_1^{\pm})^2/2a_0^{\pm}$. In this instance, the DW propagation field H_P can be defined as $H_P = |a_1^{\pm}/a_2^{\pm}|$, which is conceptually equivalent to the minimum field H_{crit} required to remove the energy barrier. Our experimental analysis reveals that the propagation field H_P exhibits $1/w$ dependence, which we ascribe to the influence of the wire edge roughness[8], with a proportionality coefficient of 4.6 Oe μm and an intercept of 25.2 Oe (Supplementary Information VI).

The activation volume V_A provides a bound on the regime of the 1D criticality. Figure 3 shows the diameter d_A of the activation volume, that is, $V_A = \pi d_A^2 t_f/4$, determined by the best fit to equation (1). Here, t_f denotes the film thickness. The figure clearly shows that there exist two distinct regimes of the wire width. For narrow wires, the activation diameter d_A equals the wire width w, as indicated by the blue line in Fig. 3, because the activation volume is extrinsically confined by the geometrical constriction[21]. A single activation volume then occupies the whole width of the wire and there remains only one possible DW motion: hopping over the activation volume along the wire as a 1D particle. On the other hand, for wide wires, the activation diameter is smaller than the wire width. For this case, the wire cross-section contains multiple activation volumes and the 1D particle picture breaks down. The crossover between the two regimes occurs at around 300 nm, in agreement with the transition between one and two dimensions as seen in Fig. 1. We therefore conclude that the activation volume in comparison with the wire width is another governing factor for dimensionality from the viewpoint of 1D criticality.

We report the experimental verification of new statistical scaling criticality in one dimension as well as the transitional behaviour from two dimensions to one. Universality exists at the criticality transition, manifesting gradual crossover behaviour between dimensions at about a few hundred nanometres. These results provide a step forward to a new scaling criticality for nanometre-sized physical structures, as yet much less examined, which are fundamental building blocks of emerging nanoscience and nanotechnologies.

METHODS SUMMARY

The scanning MOKE microscope is equipped with an objective lens (numerical aperture = 0.9) and a pulsed laser (λ = 658 nm), which provides a 440-nm laser spot. The out-of-plane component of the magnetization state is monitored by detecting the polar MOKE signal. The laser intensity at the sample is kept lower than 45 μW to avoid possible heating damage. The temperature rise at the laser spot is estimated to be less than 1 K. The phase modulation technique is adopted with a lock-in amplifier, a photo-elastic modulator, and a low-noise photodiode

with 2×10^6 V A^{-1} signal gain. The signal voltage is collected by a data acquisition board at 250 kHz. A home-built electromagnet is used to generate a magnetic field of up to 200 Oe with the rising time less than 1 ms. A large magnetic field (~200 Oe) is first applied to saturate the nanowire and then a magnetic domain is initiated by thermomagnetic writing with a magnetic field pulse (25 Oe and 3 ms) and a laser pulse (5.6 mW and 1 s) focused on a local area of the nanowires. The DW is reproducibly formed with an accuracy of ± 1 μm (± 2 μm for $w < 200$ nm). Both the MOKE signal and the magnetic field trigger signal are simultaneously detected to precisely determine the DW arrival time. All the measurements are repeated ten times. The magnetic field H is swept from 0 to 200 Oe with increments of 0.1–0.5 Oe depending on the measurable DW speed range.

1. Lux, T. & Marchesi, M. Scaling and criticality in a stochastic multi-agent model of a financial market. *Nature* **397**, 498–500 (1999).
2. Carlson, J. M., Langer, J. S. & Shaw, B. E. Dynamics of earthquake faults. *Rev. Mod. Phys.* **66**, 657–670 (1994).
3. Sethna, J. P., Dahmen, K. A. & Myers, C. R. Crackling noise. *Nature* **410**, 242–250 (2001).
4. Suki, B., Barabási, A.-L., Hantos, Z., Peták, F. & Stanley, H. E. Avalanches and power-law behaviour in lung inflation. *Nature* **368**, 615–618 (1994).
5. Blatter, G., Feigel'man, M. V., Geshkenbein, V. B., Larkin, A. I. & Vinokur, V. M. Vortices in high-temperature superconductors. *Rev. Mod. Phys.* **66**, 1125–1388 (1994).
6. Lemerle, S. *et al.* Domain wall creep in an Ising ultrathin magnetic film. *Phys. Rev. Lett.* **80**, 849–852 (1998).
7. Chauve, P., Giamarchi, T. & Le Doussal, P. Creep and depinning in disordered media. *Phys. Rev. B* **62**, 6241–6267 (2000).
8. Cayssol, F., Ravelosona, D., Chappert, C., Ferré, J. & Jamet, J. P. Domain wall creep in magnetic wires. *Phys. Rev. Lett.* **92**, 107202 (2004).
9. Metaxas, P. J. *et al.* Creep and flow regimes of magnetic domain-wall motion in ultrathin Pt/Co/Pt films with perpendicular anisotropy. *Phys. Rev. Lett.* **99**, 217208 (2007).
10. Derrida, B. Velocity and diffusion constant of a periodic one-dimensional hopping model. *J. Stat. Phys.* **31**, 433–450 (1983).
11. Bak, P., Tang, C. & Wiesenfeld, K. Self-organized criticality: an explanation of 1/*f* noise. *Phys. Rev. Lett.* **59**, 381–384 (1987).
12. Fisher, D. S. Interface fluctuations in disordered systems: 5-ε expansion and failure of dimensional reduction. *Phys. Rev. Lett.* **56**, 1964–1967 (1986).
13. Cizeau, P., Zapperi, S., Durin, G. & Stanley, H. E. Dynamics of a ferromagnetic domain wall and the Barkhausen effect. *Phys. Rev. Lett.* **79**, 4669–4672 (1997).
14. Perković, O., Dahmen, K. & Sethna, J. P. Avalanches, Barkhausen noise, and plain old criticality. *Phys. Rev. Lett.* **75**, 4528–4531 (1995).
15. Le Doussal, P. & Vinokur, V. M. Creep in one dimension and phenomenological theory of glass dynamics. *Physica C* **254**, 63–68 (1995).
16. Kim, D.-H., Choe, S.-B. & Shin, S.-C. Direct observation of Barkhausen avalanche in Co thin films. *Phys. Rev. Lett.* **90**, 087203 (2003).
17. Ryu, K.-S., Akinaga, H. & Shin, S.-C. Tunable scaling behaviour observed in Barkhausen criticality of a ferromagnetic film. *Nature Phys.* **3**, 547–550 (2007).
18. Pommier, J. *et al.* Magnetic reversal in ultrathin ferromagnetic films with perpendicular anisotropy: domain observations. *Phys. Rev. Lett.* **65**, 2054–2057 (1990).
19. Kirby, R. D., Shen, J. X., Hardy, R. J. & Sellmyer, D. J. Magnetization reversal in nanoscale magnetic films with perpendicular anisotropy. *Phys. Rev. B* **49**, 10810–10813 (1994).
20. Choe, S.-B. & Shin, S.-C. Phase diagram of three contrasting magnetization reversal phases in uniaxial ferromagnetic thin films. *Appl. Phys. Lett.* **80**, 1791–1793 (2002).
21. Skomski, R., Zeng, H., Zheng, M. & Sellmyer, D. J. Magnetic localization in transition-metal nanowires. *Phys. Rev. B* **62**, 3900–3904 (2000).

Author Contributions S.-B.C. planned and supervised the project; K.-J.K. designed and performed the experiments; C.-W.L., Y.J.C., and. S.S. prepared sample films; J.-C.L. and K.-H.S. carried out patterning process; S.-M.A. and K.-S.L. characterized the films and nanostructures; K.-J.K., S.-B.C. and H.-W.L. performed theoretical analysis and wrote the manuscript.

Author Information Reprints and permissions information is available at www.nature.com/reprints. Correspondence and requests for materials should be addressed to S.-B.C. (sugbong@snu.ac.kr) or H.-W.L. (hwl@postech.ac.kr).